Inorganic Chemistry
Article
Cite This: Inorg. Chem. 2018, 57, 12697−12708
pubs.acs.org/IC

Chiral Control in Pentacoordinate Systems: The Case of Organosilicates

Leon J. P. van der Boon,[†] Laurens van Gelderen,[†] Tim R. de Groot,[†] Martin Lutz,[‡] J. Chris Slootweg,[†,§] Andreas W. Ehlers,*[,†,§,∥] and Koop Lammertsma*[,†,∥]

[†]Department of Chemistry and Pharmaceutical Sciences, Faculty of Sciences, Vrije Universiteit Amsterdam, De Boelelaan 1083, 1081 HV Amsterdam, The Netherlands

[‡]Crystal and Structural Chemistry, Bijvoet Center for Biomolecular Research, Utrecht University, Padualaan 8, 3584 CH Utrecht, The Netherlands

[§]Van 't Hoff Institute for Molecular Sciences, University of Amsterdam, Science Park 904, 1098 HX Amsterdam, The Netherlands

[∥]Department of Chemistry, University of Johannesburg, Auckland Park, Johannesburg 2006, South Africa

Supporting Information

ABSTRACT: Chirality at the central element of pentacoordinate systems can be controlled with two identical bidentate ligands. In such cases the topological Levi−Desargues graph for all the Berry pseudorotations (BPR, max. 20) reduces to interconnected inner and outer "circles" that represent the dynamic enantiomer pair. High enough barriers of the BPR crossovers between the two circles is all what is needed to ascertain chiral integrity. This is illustrated computationally and experimentally for the organosilicates **7** and **10** that carry besides a Me (**a**), Et (**b**), Ph (**c**), or F (**d**) group two bidentate 2-(phenyl)benzo[*b*]-thiophene or 2-(phenyl)naphthyl ligands, respectively. The enantiomers of tetraorganosilane precursor **9** could be separated by column chromatography. Their chiral integrity persisted on forming the silicates. CD spectra are reported for **10c**. Fluoro derivative **10d** is shown to have its electronegative F substituent in an equatorial position, is stable toward hydrolysis, and its enantiomers do not racemize at ambient temperatures, while those of **10c** racemize slowly.

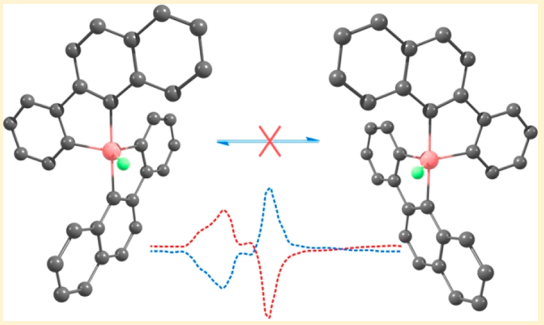

INTRODUCTION

Chirality is a cornerstone of organic chemistry and existential to all living matter. The very essence of chirality is the nonsuperimposability of molecules on their mirror images. Prevalent in most chiral molecules is the asymmetric tetravalent carbon as formulated by the first Nobel laureate, J. H. van 't Hoff.[1,2] The impact of chirality in organic synthesis, biology, medicine, polymers, and materials science alike has been monumental.[3−6] The dominant role of carbon in chiral systems is complemented by tetravalent phosphorus, silicon, sulfur, nitrogen, and boron, but chirality is not limited to molecules deduced from these elements only.[7−9]

Chirality of pentacoordinate systems is likewise of inherent importance and impacts fields like biocatalysis and asymmetric catalysis.[10] However, typically the ligands are responsible for chirality rather than the transition metal center itself, as in chiral-at-metal catalysis that has only recently come to the fore.[11,12] The simple reason for the far smaller focus on chiral pentacoordinate elements in comparison to the tetracoordinated ones is their dynamic behavior that induces racemization of enantiomers, which strongly contrast the conformational rigidity of carbon.[13]

The distinguishing feature is that pentacoordinate systems are prone to nondissociative racemization by means of the Berry pseudorotation (BPR) where both axial substituents of a trigonal bipyramid (TBP) readily exchange with two equatorial substituents (Figure 1).[14,15]

Recently though, the stereoselectivity for silicon-centered nucleophilic substitutions was shown to be controllable by selectively hampering the BPRs in the pentacoordinate

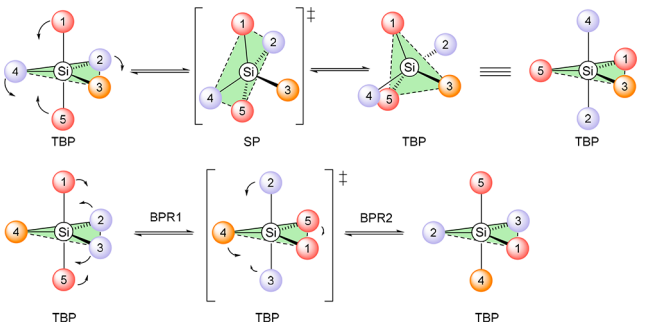

Figure 1. Berry pseudorotation (BPR, top) and Turnstile rotation (TR, bottom), which is a double BPR.

Received: July 5, 2018
Published: October 2, 2018

DOI: 10.1021/acs.inorgchem.8b01861
Inorg. Chem. 2018, 57, 12697−12708

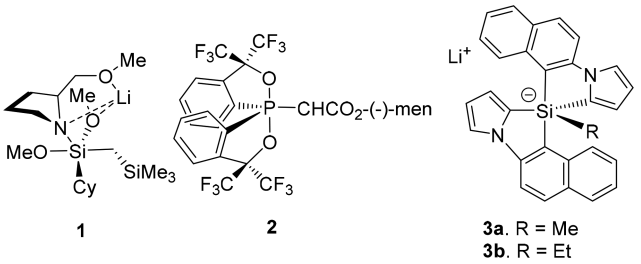

Figure 2. Pentaorganosilicate intermediate (left) and isolated phosphorane (middle; men = menthyl) and pentaorganosilicates (right).

intermediate **1** shown in Figure 2.[16] Akiba and co-workers have shown in elegant work that high epimerization barriers at phosphorus can be obtained using (only) the Martin ligand,[17−19] enabling full inhibition of a BPR as was demonstrated by chiral resolution of **2** and related molecules into their enantiomers (Figure 2).[20] An important factor of the lack of P-epimerization is the highly electronegative groups in the two axial positions; we are unaware of other related chiral phosphanes.

These two examples serve to illustrate that chiral integrity is feasible at the central element of pentacoordinate systems but also show that it is not evident how to accomplish this. In fact, the examples might be misleading if apicophilicity is used as a guiding principle. This then begs the question of how to achieve chiral integrity for pentacoordinate systems by design. Here we present the principles how to obtain chiral pentaorganosilicates without the use of chiral ligands.[21] As silicates have modest pseudorotation barriers, smaller than those for phosphanes, Martin's ligand does not hamper the BPR in silicates sufficiently to enable rigidity.[22] We provide the conditions needed to obtain any chiral pentacoordinate systems and present the first chiral pentacoordinate silicon species with chirality only on the central silicon atom.

The starting point is to recognize how to interfere into the dynamic conformational behavior of pentacoordinate systems. Earlier, we reported in detail on the pseudorotations of pentaorganosilicates and pentacoordinate transition metal complexes.[23] For clarity and consistency, we summarize and expand on the findings of this work in order to pinpoint the approach to achieve chiral integrity.

All feasible pseudorotations for a silicate with five different substituents can be summarized in a topological Levi−Desargues graph (Figure 3a), which is the starting point for our design approach.[23−25] Such a system has, in fact, 20 possible trigonal bipyramidal (TBP) conformations. These are represented by dots in the Levi−Desargues graph with the numbers symbolizing the two axial ligands, such as the enantiomeric pair 15 and 51. Each line in the graph represents a BPR. At a minimum, five such sequential pseudorotations are required for racemization to occur for any (Δ and Λ) enantiomeric pair. Inhibiting just one of the BPRs does not suffice, because there are ample sequences (paths) that connect the enantiomeric pairs. Controlling all of these daunting task and simplifications are needed.

The complexity of the Levi−Desargues graph reduces considerably on using two identical bidentate ligands. This is illustrated for reported silicate **4**, which possesses two 1-phenylpyrrole-2,2′-diyl units and a methyl group (Figure 3b).[26] The number of TBP conformations for this silicate reduces from 20 to 16 or by two for each bidentate ligand. The simple reason being that one phenylpyrrole group cannot occupy both

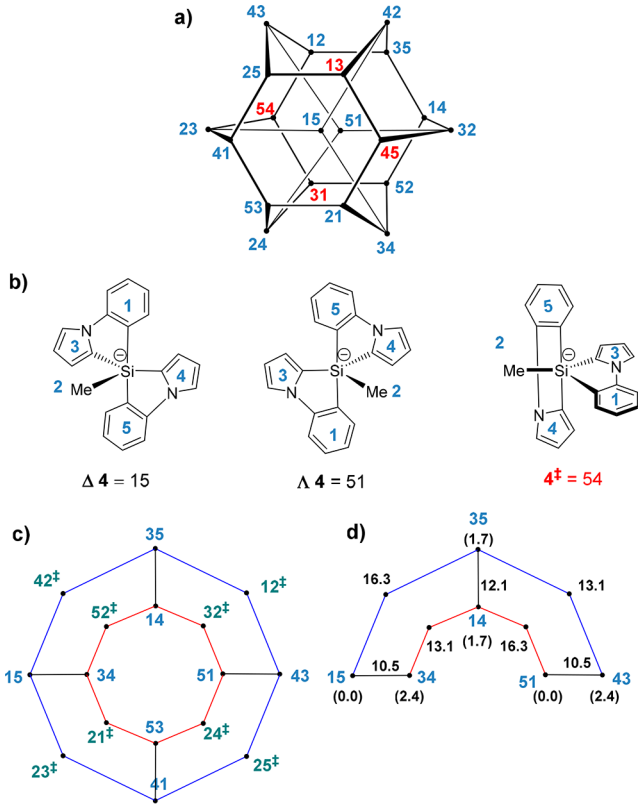

Figure 3. (a) Levi−Desargues graph for Berry pseudorotations of pentacoordinate systems. Unfeasible biaxial conformations for **4** are red. (b) Two most stable conformations of **4** and unfeasible biaxial conformation 54 (right). (c) Simplified graph for systems with two identical bidentate ligands as for **4**. Green labeled conformations are transition structures. The enantiomeric rings are shown in blue and red, respectively; only TBP conformations are shown. (d) A further simplified graph for **4** showing only conformational minima is given in blue, and their relative energies (in parentheses) and conversion barriers are in black in kcal mol^{-1}.

axial positions simultaneously. Thus, TBP conformer 15 with the axial phenyl group (labeled 1) and the equatorial pyrrole group (labeled 5) cannot stereopermutate to TBP conformer 13 and neither can its enantiomer 51 to conformer 31. The same applies for the other phenylpyrrole group that inhibits formation of conformers 54 and 45 (see Figure 3b, right). Eliminating these four (labeled in red) from the Levi−Desargues graph reduces it to two interconnected double circles (Figure 3c). The outer one (colored blue) represents one-half of the dynamic enantiomeric pairs (including Δ-15) and the inner circle (colored red) contains the enantiomeric counterpart; the two circles are interconnected by four BPR crossovers. With both bidentate ligands being identical, only half of the reduced graph needs to be considered for symmetry reasons, reducing the number of crossovers to consider (Figure 3d). This simplified representation reveals three different pathways for racemizing conformers Δ-15 and Λ-51 with each comprising five subsequent BPRs (i.e., Δ-15 ⇄ Λ-35 ⇄ Δ-43 ⇄ Λ-51, Δ-15 ⇄ Λ-35 ⇄ Δ-14 ⇄ Λ-51, and Δ-15 ⇄ Λ-34 ⇄ Δ-14 ⇄ Λ-51). All three pathways require barriers high enough to prevent racemization. The computed values at B3LYP/6-311++G(2d,p) make clear that this is not the case for **4** (see values in black in Figure 3d).[11]

The task of designing silicates with chiral integrity then is to determine which BPRs need to be influenced to inhibit all three racemization pathways. The clearest choice is to increase

DOI: 10.1021/acs.inorgchem.8b01861
Inorg. Chem. 2018, 57, 12697−12708

the two different crossover barriers between the Δ and Λ enantiomeric rings (blue and red in Figure 3c,d) Extending the size of the bidentate ligands to induce friction in the pseudorotations is an obvious approach to accomplish this. In fact, we have attempted this earlier for **3** (Figure 2), which can be viewed as extended **4**, but it did not lead to the desired result.[27] However, two diastereotopic CH_2 hydrogen atoms could be observed at −50 °C for the ethyl group of **4b**, suggesting only limited conformational rigidity at that low temperature or below. All attempts to achieve separation of racemic **4** into its enantiomers were to no avail. Clearly, a still more focused approach was needed to obtain stable chiral silicates experimentally.

We choose to replace the pyrroles in **3** for phenyl groups and the naphthyls of **10** for benzo[*b*]-thiophene groups (**7**). The steric effect of Ph-catenated 6-membered phenyl groups on the silicate is expected to differ from that with the Ph-catenated 5-membered thiophene groups because of their different spatial orientations, which should give insight into the demands for chiral integrity. Exploring these choices of silicates computationally and experimentally reveal examples of what is needed to achieve chiral integrity at room temperature. We will further show that chiral silicates **10** can be obtained by phenylation/fluorination of their chiral tetracoordinate silane precursors.

RESULTS AND DISCUSSION

A computational survey for **7** and **10** is presented first to evaluate their potential as silicates with chiral integrity, which is then followed by a description of their synthesis and chiral properties.

Computational Design. The potential energy surfaces for both **7** and **10** were examined at B3LYP-GD3/6-311++G(2p,d)//B3LYP/6-31G(d). This method has shown to give good agreements for related, simpler cases;[26−29] dispersion correction was added to account for possible π/π interactions.[30] We start by analyzing the data for **7a**, which carries a methyl group and two bidentate 2-(phenyl)benzo[*b*]thiophene ligands. Figure 3b gives the numbering scheme of all the Si-substituents with the TBP conformers labeled by their axial ones. Three enantiomeric minima were identified of which the Δ-15/Λ-51 pair is energetically favored over the Λ-35/Δ-14 and Δ-43/Λ-34 pairs by 3.4 and 6.9 kcal mol^{-1}, respectively (Figure 4). The upper part of Figure 4 shows the minima (Δ-15 ⇄ Λ-35 ⇄ Δ-43) that are on the "outer" ring of the topological graph in Figure 3c,d, and the bottom part shows those of the "inner" ring (Λ-34 ⇄ Δ-14 ⇄ Λ-51). The identical (enantiomeric) BPRs paths Δ-15 ⇄ Λ-34 and Δ-43 ⇄ Λ-51 that connect the outer and inner halves of Figure 3d have the anticipated large barrier (23.9 kcal/mol) due to steric obstruction, as the *ortho*-hydrogens of the phenyl and benzo[*b*]thiophene moieties of the two bidentate ligands cannot pass each other unimpeded in the square planar (SP) transition state (TS); the barrier is similar to that of 26.6 kcal mol^{-1} computed for **3**.[27] The other BPR path, connecting the enantiomeric minima Λ-35 and Δ-14, is traversed if the two benzo[*b*]thiophene moieties can pass each other in the square planar TS. However, this motion is obstructed, so significant that the expulsion of one of the substituents is preferred instead. The barrier for single Si−C bond cleavage of 30.7 kcal mol^{-1} concurs with earlier analyses of pentaorganosilicates.[27] With only high energy barriers connecting the TBPs of the outer and inner halves of Figure 3d, racemization of chiral **7a** may be subdued at room temperature.

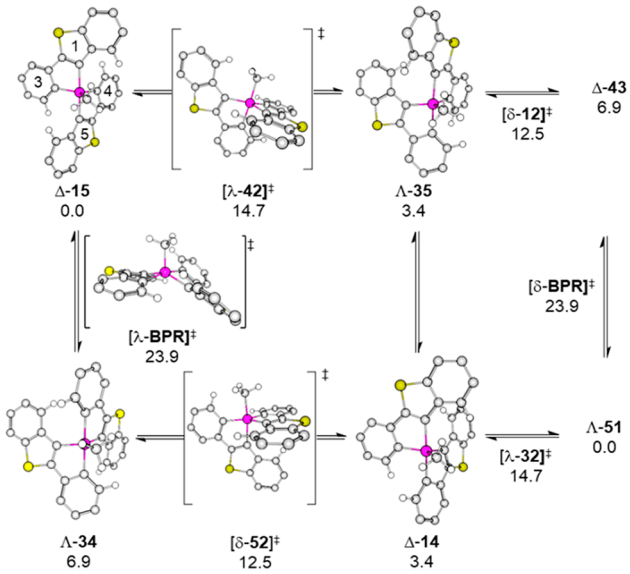

Figure 4. Racemization scheme for methyl,bis-2-(phenyl)-benzothiophene silicate **7a** at B3LYP-GD3/6-311++G(2p,d)//B3LYP/6-31G(d).

Racemization may then be hampered, and each enantiomer can still show dynamic behavior if the barriers for connecting the minima on both the upper and lower parts of Figure 4 are modest, which seems to be the case. Namely, the one for converting Δ-15 into Λ-35 amounts to "only" 14.7 kcal mol^{-1} and involves a Turnstile rotation (TR), which is a single-step double BPR[23,31] with [λ-42]‡ as the TBP transition structure. Also, the subsequent conversion of Λ-35 (3.4 kcal mol^{-1}) to the least stable pseudorotamer Δ-43 (6.9 kcal mol^{-1}) has a modest barrier of 12.5 kcal mol^{-1} with TBP [δ-12]‡ as TS (Figure 4, upper part). Of course, the entire process is mirrored for Λ-34 ⇄ Δ-14 ⇄ Λ-51 with [δ-52]‡ and [λ-32]‡ as respective TSs. Thus, whereas each enantiomer may be subject to dynamic behavior in solution at room temperature, it is still expected that NMR will reveal mainly the most abundant conformer for **7a**, i.e., Δ-15 and/or Λ-51.[27]

Next we turn to the structures and energies of naphthalene congener **10** (**a**: Me; **c**: Ph; **d**: F) given in Figure 5 using the same level of theory; **10b** (Et) is omitted due to its similarity to **10a**. Displayed are the Δ-15 ⇄ Λ-35 ⇄ Δ-43 stereopermutations of the outer ring of Figure 3c, (analogues to the upper part of Figure 4 for **7a**) and the Δ-43 ⇄ Λ-51 (crossover) path connecting it to the inner ring. Altogether, it constitutes one of the enantiomeric routes for racemizing Δ-15 and Λ-51, which has, however, a prohibitively high barrier of 27.7 kcal mol^{-1} for methyl-containing silicate **10a** and even 33.7 kcal mol^{-1} for fluoro silicate **10d**. These barriers are even higher than the corresponding ones discussed for bis-2-(phenyl)benzo[*b*]thiophene analogue **7a** (24.5 kcal mol^{-1}; Figure 4) and pyrrole-based **3** (26.6 kcal mol^{-1}).[27]

Evidently and as expected, the transition states experience more friction between the α-hydrogens of the two bidentate naphthyl ligands than for the two benzo[*b*]thiophenes. The barrier for the BPR conversion of Δ-43 into Λ-51 is hardly affected by changing the size of the "fifth" substituent from a methyl (**10a**: 27.7 kcal mol^{-1}) to a phenyl group (**10c**: 28.8 kcal mol^{-1}). The other potential racemization route that involves Λ-35 ⇄ Δ-14 could not be established as cleavage of the Si−C bond occurred instead.

DOI: 10.1021/acs.inorgchem.8b01861
Inorg. Chem. 2018, 57, 12697−12708

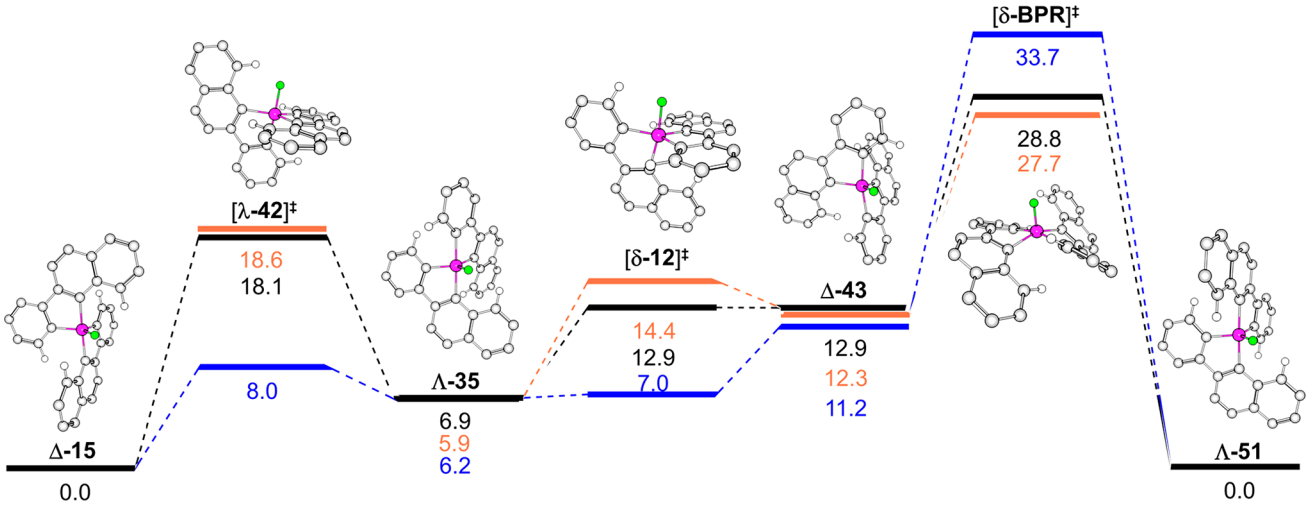

Figure 5. Racemization scheme of methyl,bis-2-(phenyl)naphthylsilicate **10a** (orange) and corresponding phenyl **10c** (black) and fluorine **10d** (blue) analogues at B3LYP-GD3/6-311++G(2p,d)//B3LYP/6-31G(d).

Whereas racemization may be inhibited, the enantiomers of naphthylsilicate **10** can display dynamic behavior but to a lesser extent than discussed for the benzo[*b*]thiophene homologue **7a** for two reasons. First, the Turnstile rotation barrier ([λ−42]‡) of 18.1 (18.6) kcal mol^{-1} for converting Δ-15 into Λ-35 for **10a** (**10c**) is much higher than the 14.7 kcal mol^{-1} value for **7a**. Second, the energy differences of the Δ-15/Λ-51 pair for **10a** (**10c**) with the other Λ-35/Δ-14 and Δ-43/Λ-34 minima of 5.9 (6.9) and 12.3 (12.3) kcal mol^{-1}, respectively, are much larger than those for **7a** (Figure 4). Consequently, it is expected that only Δ-15/Λ-51 can be observed in solution.

Electronic effects can also play an important role as is evident on replacing the methyl group of silicate **10a** for a fluorine substituent (**10d**). As noted, the barrier for the Δ-43 ⇄ Λ-51 conversion increases significantly, which is due to the destabilizing effect of the apical fluorine in the square planar TS. In contrast, and as expected, the barriers for the Δ-15 ⇄ Λ-35 ⇄ Δ-43 Turnstile rotations are much reduced with fluorine in the apical position of the TBP transition structures [λ−42]‡ and [δ-12]‡. In contrast to **10a** where the bis-equatorial naphthalene ring is π-donating into the Si-Me antibonding orbital, thereby raising its energy,[32] the barriers are much reduced with the stabilizing apical fluorine (**10d**). The effect is most pronounced for conformer δ-12, which in fact becomes a local energy minimum. Its energy difference of 0.8 kcal mol^{-1} with Λ-35 was too small to determine a barrier, nor could the barrier be found for the formation of conformer Δ-43, which is likely also very small. In fact, Δ-43 is a transition state for **10d**, but a suitable minimum between this TS and the single Berry TS (δ-BPR) could not be established. Be that as it may, the dynamics of the enantiomers of fluorosilicate **10d** seems to be more pronounced than for alkyl and phenyl derivatives **10a** and **10c**. Quite interestingly, the global minimum Δ-15 has its electronegative fluorine substituent in an equatorial instead of an axial position.[27,33]

Synthesis and Characterization. We now proceed with the synthesis of silicate **10** first and then **7**, following an established procedure.[29] The synthesis of **10** starts with 2-(2-bromophenyl)-1-bromonaphthalene **8** (Scheme 1) obtained by a Suzuki coupling between 1-bromo-2-naphthyl triflate and *ortho*-bromophenylboronic acid. Whereas this coupling reaction usually performs better with bromides,[34] we suspect that

Scheme 1. Synthesis of Sterically Encumbered Silicates

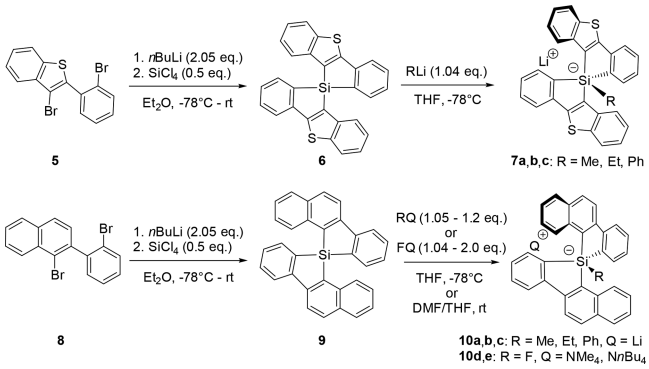

in this case steric factors may favor the triflate despite its low conversion (35% yield) and the formation of palladium black. Dilithiation of dibromide **8** followed by reaction with $SiCl_4$ afforded bis(2-phenylnaphthalene-2,1′-diyl)silane **9** in 70% yield. Further alkylation with MeLi or EtLi, arylation with PhLi, or fluorination with Me_4NF or nBu_4NF yielded corresponding silicates **10a**−**e** in almost quantitative yields. The synthesis of **7** resembles that of **10** and starts with 3-bromo-2-(2-bromophenyl)benzo[*b*]thiophene (**5**, Scheme 1), which was obtained in 79% yield by a Suzuki coupling of 2,3-dibromobenzo[*b*]thiophene and *ortho*-bromophenylboronic acid. Treatment of dilithiated **5** with $SiCl_4$ gave silane **6**[35] from which silicates **7a**−**c** were formed by reaction with MeLi, EtLi, or PhLi. Asymmetric synthesis of the spirosilane precursors have been described elsewhere.[36]

The formation of the silicates from the silanes can be monitored conveniently by ^{29}Si NMR spectroscopy due to the ca. 90 ppm upfield shift of the Si-resonance. Illustrative are the 87.6 ppm for **7a** (δ −111.7; cf., silane **6** δ −24.1) and that of 86.4 ppm for **10a** (−95.0; cf., silane **9** −8.6). The presence of the fluorine atom in **10d** is evident from the doublet of 287.8 Hz in both its ^{29}Si (δ −81.3) and ^{19}F NMR (δ −110.0) spectra; this ^{1}J(Si,F) coupling is identical, 287.0 Hz, for **10e** since both anions are equivalent. These large coupling constants can be attributed to the fluorine's equatorial position in the silicate,[27] which would suggest that in solution mainly (or merely) the Δ-15/Λ-51 conformational pair is observed. In this context, it

DOI: 10.1021/acs.inorgchem.8b01861
Inorg. Chem. 2018, 57, 12697−12708

is relevant to note that for each silicate **10a−e** and **7a−c**, only a single ^{29}Si NMR resonance was observed, which we assign to the preferred 15/51 conformers, in concurrence with the computational results and the sizable energy difference with their stereoisomers.

The ^{1}H NMR spectra of ethyl substituted **7b** and **10b** provide support for their conformational rigidity in solution, namely, both show diastereotopic methylene protons. The assignment of the axial and equatorial CH_2 protons can be derived from the coupling with carbons 1 and 2 (see Figure 6). The ethyl

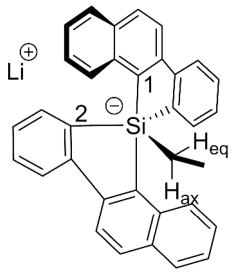

Figure 6. Silicate **10b** with diastereotopic CH_2 protons.

group appears to be an excellent diagnostic tool for determining conformational rigidity. Dynamic silicates like **4**-Et give a coalesced CH_2 signal at ambient temperatures,[11], but like **3b** (Figure 2), the methylene resonances for more rigid **7b** and **10b** do not even coalesce at 50 °C, which indicates a barrier of at least 21 kcal mol^{-1}. While coalescence may then not be observed on the NMR time scale, exchange experiments (2D-EXSY) do show the two diastereotopic protons to be correlated at ambient temperatures. This can be attributed to the modest barriers for the exchange of conformers 15/51, 35/14, and 43/34 with concurrent rotations of the axial and equatorial CH_2 protons. These results give comfort to the notion that conformational rigidity can be obtained by inhibiting a single BPR. In earlier reported **3b**, a Turnstile rotation was inhibited,[27] which seemingly is not needed to prevent racemization (vide infra).

Single crystal X-ray structure determinations were performed for phenyl containing silicate **7c** [racemate] and fluorine substituted **10e** [enantiopure]. Their molecular structures, displayed in Figure 7, reveal similar TBP conformations with the two benzo[*b*]thiophene groups of **7c** and the two naphthyl groups of **10e** in axial positions. As a consequence, the connecting phenyl substituents occupy two of the three equatorial positions in both structures, but although these groups would ideally have a parallel alignment with the axial bonds for maximum π stabilization,[32] the twist angles of 44.3(14)° for **7c** and 48.8(2)° for **10c** reflect steric congestion between the phenyl's *ortho*-hydrogen and the α-hydrogens of the benzo[*b*]thiophene and naphthyl groups, respectively. Both molecular structures closely resemble the DFT computed ones for the Δ-15/Λ-51 conformers of **7c** and **10e** and thereby give credence to these being the global energy minima. As noted, this is quite a remarkable observation for **10e** as it has the fluorine substituent in an equatorial position, whereas the dogma is that such a strong electron-withdrawing substituent should occupy an axial position. The preference for the equatorial position of the fluorine atom originates from axial−equatorial aromatic ring systems, which would otherwise be in the bis-equatorial position and cause unfavorable π-interaction with the axial bonds.[32] Moreover, silicates bearing the SiC_4F motif have so far only been observed in solution or as transient species.[27,37−39]

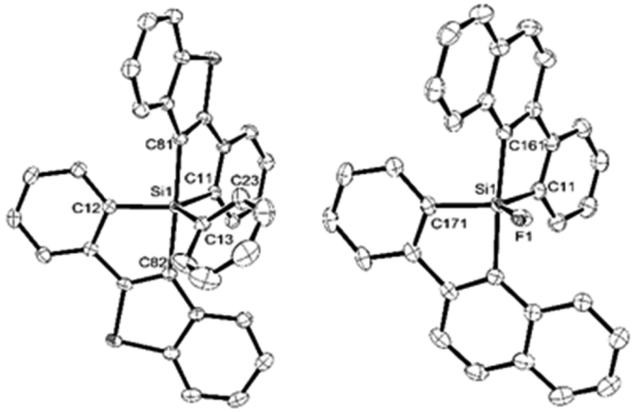

Figure 7. Molecular structures of **7c** (left) and **10e** (right) in their crystals (ellipsoids are set at 50% probability; hydrogen atoms, lithium counterion and THF solvent molecules (**7c**), DCM molecule, and N*n*Bu$_4$ counterion (**10e**) are omitted for clarity). Selected bond lengths [Å] and angles and torsion angles [°] for **7c**: Si1−C82 2.0363(13), Si1−C11 1.9395(13), Si1−C13 1.9247(14), C13−Si1−C11 120.34(6), C13−Si1−C81 92.51(5), C11−Si1−C12 121.50(5), C11−Si1−C82 94.52(5), C23−C13−Si1−C11 44.26(14). Selected bond lengths [Å] and angles and torsion angles [°] for **10e**: Si1−C161 1.990(3), Si1−C171 1.921(3), Si1−F1 1.684(2), F1−Si1−C171 121.39(13), F1−Si1−C161 88.15(12), C171−Si1−C11 115.80(15), C171−Si1−C161 97.97(14).

The surprisingly stability of silicate **10e** with its equatorial fluorine substituent and *n*Bu$_4$N$^+$ as counterion is further highlighted by its resilience to hydrolysis, showing only slow decomposition in water at a rate of about 10%/h. This behavior is stunningly different from all other organosilicates, which are typically extremely sensitive to moisture.[28] Only few hydrolytically stable ones are known.[40] Upon hydrolysis of phenyl lithium silicate **10c**, one of its axial bonds cleaves to yield **11** (90−95% pure) as deduced from the change in mass, the change in ^{29}Si NMR shift from −99.47 to −10.40 ppm, and the appearance of a singlet in the aromatic region that is assigned to H1 (Figure 8).

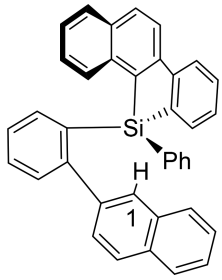

Figure 8. Hydrolysis product **11** from **10c**.

It is noteworthy that the counterion markedly influences the solubility of the silicates. For example, Li$^+$ salts **10a−c** are soluble in both THF and DMF, but Me$_4$N$^+$ salt **10d** is only soluble in DMF. *n*Bu$_4$N$^+$ salt **10e** dissolves in THF, DCM, and even Et$_2$O.

Chiral Silicates. Our next step was to demonstrate chiral integrity for one of the organosilicates. On the basis of the computed racemization barriers for **10** being higher than those for **7** as well as on the NMR spectroscopic analyses of their ethyl derivatives, we decided **10** had the best chance to establish chiral integrity.

We started by separating bis(2-phenylnaphthalene-2,1′-diyl)silane **9** into its enantiomers with chiral preparative

DOI: 10.1021/acs.inorgchem.8b01861
Inorg. Chem. 2018, 57, 12697−12708

HPLC. The molecular structure of Δ-**9** [enantiopure], obtained from a single crystal X-ray structure determination, is shown in Figure 9. The circular dichroism spectra for both

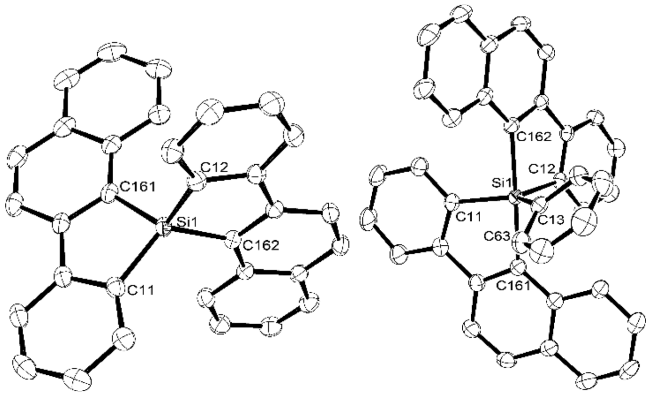

Figure 9. Molecular structures of Δ-**9** (left) and Λ-**10c** (right) in their crystals (ellipsoids are set at 50% probability; hydrogen atoms, lithium counterion and THF solvent molecule (Λ-**10c**), are omitted for clarity). Selected bond lengths [Å] and angles and torsion angles [°] for Δ-**9**: Si1−C161 1.8705(15), Si1−C11 1.8607(16), C161−Si1−C11 91.94(7), C161−Si1−C162 118.37(7), C11−Si1−C12 119.45(7), C11−C61−C71−C161−2.79(19). Selected bond lengths [Å] and angles and torsion angles [°] for Δ-**10c**: Si1−C162 2.030(2), Si1−C12 1.929(2), Si1−C13 1.927(3), C11−Si1−C13 127.77(11), C162−Si1−C13 90.03(10), C11−Si1−C12 114.67(11), C11−Si1−C162 94.21(10), C162−Si1−C13−C23−48.80(2).

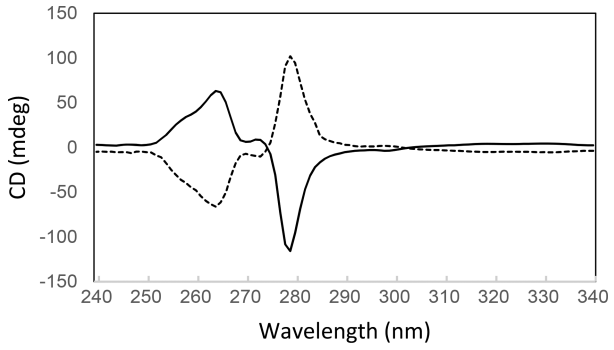

Figure 10. CD spectra of Δ-**9** (solid line) and Λ-**9** (broken line) in THF (5.6×10^{-5} M).

enantiomers in THF solutions are displayed in Figure 10 and show the expected opposite Cotton effects with two distinct maxima at 264 and 279 nm, suggesting high optical purity, which is in good agreement with the >99% ee observed in chiral HPLC. As expected, there is no sign of racemization under ambient conditions. Both silane enantiomers were then transformed to chiral **10a,c,d** silicates using the described procedure (vide supra). Crystals suitable for a single crystal structure determination were obtained for Λ**10c**. Its molecular structure is given in Figure 9 and shows chiral integrity in the solid state. Note that the chiral signature changes from Δ for tetra-coordinate silane **9** to Λ for penta-coordinate silicate **10**. Silicate Λ-**10c** has a structure similar to **7c** and **10e** with the phenyl substituent skewed to the axial bond. The structure compares well with the DFT computed one for the Λ-15. To establish whether the chiral integrity is also maintained in solution we recorded the CD spectra for both enantiomers of **10c** in THF solutions (Figure 11).

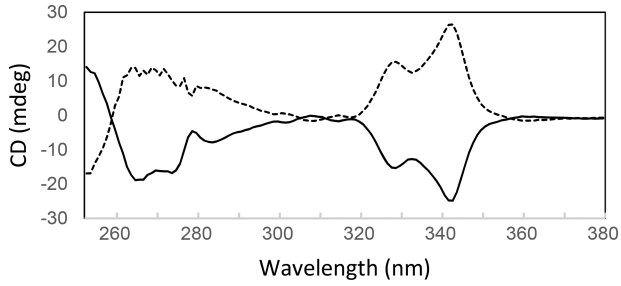

Figure 11. CD spectra of Δ-**10c** (solid line) and Λ-**10c** (dashed line) in THF (1.9×10^{-4} M) both measured 30 min after their synthesis.

The CD spectra of the enantiomers of **10c** show maxima at 266 and 274 nm, akin to **9** but with the same sign, and two new distinct maxima at 329 and 343 nm, also with the same sign. The spectra of Λ-**10c** and Δ-**10c** show opposite chirality with the same magnitude for the maxima, thereby suggesting high optical purity for these enantiomers at ambient temperature. The same was attempted for silicate **10a**, which carries a methyl group instead of a phenyl group. On treating silane Λ-**9** with MeLi, the expected product was silicate Δ-**10a**, but a CD absorption was absent upon measurement after 30 min, which was the time needed for sample preparation. The most logical explanation is that Δ-**10a** undergoes fast racemization in solution, albeit that the computational results (no solvation effects included) show only a 1.1 kcal mol^{-1} lower barrier for the racemization barrier (Δ-43 ⇄ Λ-51; Figure 5) than for **10c**. Another explanation is that the reaction of MeLi is not as stereoselective as the one with the bulkier PhLi, causing racemization during the addition.

To assess whether the chiral stability of Δ-**10c** in solution is also limited at ambient temperatures, we monitored its CD spectrum in 10 min intervals, which revealed that the intensity of the spectrum was reduced by about 50% after a 1 h period (Figure 12). We attribute this decrease to a slow Berry

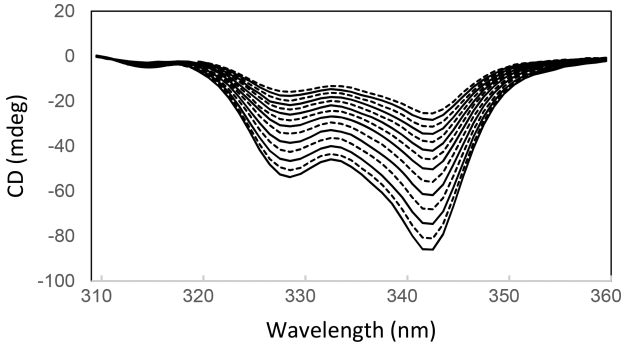

Figure 12. CD spectra of Δ-**10c** in THF (6.1×0.10^{-4} M), shown at 10 min intervals. First measurement started 30 min after synthesis of compound.

pseudorotation for the highest accessible barrier (Δ-43 ⇄ Λ-51). In a separate experiment, Λ-**10c** was stirred for 1 day at room temperature, after which no CD signals could be detected. These observations indicate that **10c** undergoes slow racemization, which is consistent with the computational results.

Interestingly, when phenyl silicate **10c** was hydrolyzed after stirring half an hour at room temperature, isolated hydrolysis product **11** retained chiral information as shown by the CD spectra of both enantiomers (Figure 13) with an ee of 33−37% as determined by HPLC. However, chiral silicates **10c**

DOI: 10.1021/acs.inorgchem.8b01861
Inorg. Chem. 2018, 57, 12697−12708

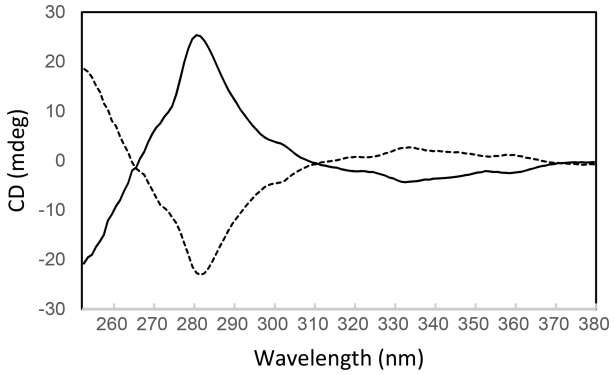

Figure 13. CD spectra of *S*-**11** and *R*-**11** in THF (1.9×10^{-4} M). Their absolute conformation could not be determined.

progressively racemize over time, and no ee or CD absorption was observed when they were reacted toward **11** after stirring overnight. This observation is in line with the progressive decline of chiral information for Δ-**10c** (Figure 12).

We conclude with silicate **10d** with its equatorial fluorine substituent. Its computed barrier of 33.7 kcal mol^{-1} for racemization (Δ-15 ⇄ Λ-51) is a significant 4.9 kcal mol^{-1} higher than that for **10c**. Figure 14 shows the CD spectra with a maximum at

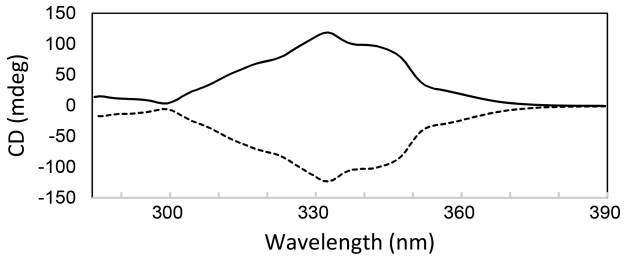

Figure 14. CD spectra of Λ-**10d** (solid line) and Δ-**10d** (broken line) in DMF (8.4×10^{-4} M).

333 nm for both enantiomers of the fluoride containing silicate; because of the DMF solvent used, the spectra could only be recorded down to 285 nm. Monitoring the spectra over time (>1 day) had no influence on the intensity of the signals. This observation indicates that silicate **10d** does not undergo racemization and displays chiral integrity at ambient temperatures.

This very fact is in itself rather remarkable. Silicate **11d** with its two all-carbon bidentate ligands and a single fluoride substituent is the most stable one of those investigated in this study. Additionally, it carries the electronegative fluoride in an equatorial position instead of an axial one. Moreover, the enantiomers of **10d** are stable and do not racemize!

Achieving a feat like this bodes well for controlling the chirality of many more penta-coordinate systems. This systematic study shows it to be well within the realm of possibilities. It reveals, even for a fluorosilicate, that chiral integrity can be maintained for higher coordinate systems in spite of the dynamic behavior of its enantiomers. We feel that the principles presented herein for stable silicates with chiral integrity serve as the onset to a much broader investigation in search of taking advantage of the inherent chirality of higher coordinate systems and to open up new opportunities and applications that have been dormant for too long.

■ CONCLUSION

In summary, we have shown for the element silicon that the chirality at the central element of pentacoordinate systems can be controlled with two identical bidentate ligands. For such systems the number of 20 possible trigonal bipyramidal structures in the topological Levi−Desargues graph reduces to 16 in two interconnected rings with each ring representing one enantiomer of the conformationally dynamic enantiomeric pairs. The two unique crossover paths connecting the two rings must be inhibited to prevent racemization. The barrier for these two Berry pseudorotations can be readily increased by extending the size of the bidentate ligands. We have demonstrated this computationally and experimentally for organosilicates **7** and **10** that carry besides a Me (**a**), Et (**b**), Ph (**c**), or F (**d**) group two bidentate 2-(phenyl)benzo[*b*]thiophene and 2-(phenyl)naphthyl ligands, respectively. Racemic neutral silane precursor **9** could be separated into its enantiomers by column chromatography. Their chiral integrity persisted on forming the organosilicates. CD spectra were obtained for **10c**, albeit that the solvated enantiomers underwent slow racemization over time. This loss of chiral information was also observed in the hydrolysis product of **10c** as the ee decreased progressively when **10c** was allowed to stir longer prior to the addition of water. In sharp contrast, fluoro derivative **10d**, which has its electronegative F group in an equatorial position, did not show any tendency to hydrolyze nor did its enantiomer show any indication for racemization.

We believe that the principles outlined in this study are applicable to any pentacoordinate system with nondissociating ligands and may advance, e.g., chiral-at-metal catalysis for asymmetric reactions and our general understanding of racemization in silicon substitution reactions.

■ EXPERIMENTAL SECTION

Computational Methods. All calculations were performed using Gaussian09D.[41] Geometries were optimized at the B3LYP/6-31G(d) level.[42−52] The nature of each stationary point was confirmed by a frequency calculation. Single-point energies were calculated at the B3LYP/6-311++G(2d,p) using GD3 as a dispersion correction.[30]

General. Pyridine was dried using activated molecular sieves (3 Å); dimethylformamide (DMF) was bought predried from Sigma-Aldrich and stored on activated molecular sieves (3 Å). Tetrahydrofuran (THF) was distilled subsequently from $LiAlH_4$ and sodium/potassium alloy and diethyl ether from sodium/potassium alloy. *n*-Butyllithium and methyllithium were purchased as 1.6 M solutions in hexanes and in diethyl ether, respectively; ethyllithium was purchased as a 0.5 M solution in benzene/cyclohexane (9:1). Phenyllithium was purchased as a 1.9 M solution in di-*tert*-butyl ether. Tetrachlorosilane was distilled and refluxed before use to remove HCl. The mass, NMR, and melting point samples of silicates were prepared and handled in the purified N_2 atmosphere of an MBRAUN Unilab glovebox; other syntheses were performed using standard Schlenk techniques. NMR spectra were recorded on a Bruker Avance 400 (^{1}H, ^{13}C, ^{29}Si, 2D spectra), or Bruker Avanve 500 (^{1}H, ^{13}C). NMR chemical shifts are internally referenced to the solvent for ^{1}H (DMF: 2.92, $CHCl_3$: 7.26, THF: 3.58, CH_2Cl_2: 5.32, DMSO: 2.50 ppm) and ^{13}C (DMF: 34.89, $CHCl_3$: 77.16, THF: 67.58, CH_2Cl_2: 53.84, DMSO: 39.52 ppm) and externally for ^{29}Si (TMS) and ^{19}F ($CFCl_3$). Melting points were measured on samples in sealed capillaries and are uncorrected. HR-ESI-MS measurements of silicates were measured on a Varian IonSpec FT-ICR mass spectrometer. CD measurements were performed on a Chiralscan CD spectrometer, using a 1 mm cuvette modified for Schlenk techniques. CD of the silicates was measured half an hour after evaporation of solvent, the silicates were dissolved in THF or DMF and the solution not used for CD was measured using NMR to establish purity. Separation of enantiomers was performed at Syncom Groningen at a preparative scale (500 mg) on a Chiralpak IA column yielding 195 mg and 145 mg of the single

DOI: 10.1021/acs.inorgchem.8b01861
Inorg. Chem. 2018, 57, 12697−12708

enantiomers with >99% ee. Chirality was determined using X-ray crystallography.

Synthesis. *3-Bromo-2-(2-bromophenyl)benzo[b]thiophene (**5**).*[16]

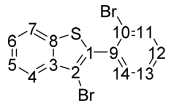

Using the method from Lammertsma et al., a solution of 2,3-dibromobenzo[*b*]thiophene[53] (5.0 mmol, 1.46 g, 1.0 equiv), 2-bromophenyl-boronic acid (5.0 mmol, 1.00 g, 1.0 equiv), $Pd(PPh_3)_4$ (0.25 mmol, 289 mg, 0.05 equiv), and Na_2CO_3 (7.5 mL, 15 mmol, 2 M in water, 3 equiv) in 50 mL of 1,4-dioxane was heated to 100 °C and stirred overnight (18 h) under nitrogen atmosphere, resulting in a black suspension. The solvent was removed under reduced pressure and the residue dissolved in DCM. The reaction mixture was washed with water and brine, and the organic layer was dried over $MgSO_4$, filtered, and concentrated *in vacuo*, resulting in a yellow oil. The oil was purified via flash column chromatography (*c*-hexane), resulting in an oil. After 3 days, white crystals were formed at 21 °C (1.44 g, 3.9 mmol, 78%). ^{1}H NMR (500.23 MHz, CD_2Cl_2, 294 K): δ = 7.88 (d, ^3J(H,H) = 8.0 Hz, 2H; H4, H7), 7.74 (d, ^3J(H,H) = 8.0 Hz, 1H; H14), 7.53 (t, ^3J(H,H) = 7.5 Hz, 1H; H5), 7.48−7.43 (m, 3H; H6, H11, H12), 7.37 (t, ^3J(H,H) = 7.5 Hz, 1H; H13). ^{13}C{^{1}H} NMR (125.78 MHz, CD_2Cl_2, 296 K): δ 138.76 (C8), 138.17 (C3), 137.77 (C9), 134.35 (C1), 133.35 (C14), 132.92 (C11), 131.20 (C13), 127.72 (C12), 126.17 (C6), 125.71 (C5), 124.79 (C10), 123.82 (C4), 122.72 (C7) 108.76 (C2).

*Benzothiophenesilane (**6**).*

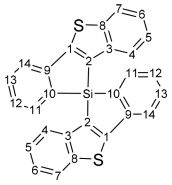

*n*BuLi (16.7 mL, 26.7 mmol, 4.1 equiv) was added to a solution of **7** (4.8 g, 13.0 mmol, 2.0 equiv) in Et_2O (55 mL) at −78 °C, and the yellow suspension was stirred at this temperature for 1 h. The reaction mixture was warmed up to room temperature, and $SiCl_4$ (6.5 mmol, 0.75 mL, 1.0 equiv) was added at 0 °C. The resulting white suspension was stirred overnight (17 h) at room temperature. The reaction mixture was washed using water and extracted three times into Et_2O. The combined organic layers were dried over $MgSO_4$, filtered, and concentrated *in vacuo*. The resulting colorless solid was further purified using flash column chromatography (*c*-hexane), which after evaporation of all volatiles resulted in a slightly yellow powder (2.03 g, 4.56 mmol, 70%). ^{1}H NMR (500.23 MHz, CD_2Cl_2, 294 K): δ 7.89 (d, ^3J(H,H) = 8.0 Hz, 2H; H7), 7.68 (d, ^3J(H,H) = 7.5 Hz, 2H; H14), 7.52 (t, ^3J(H,H) = 7.5 Hz, 2H, H13), 7.39 (d, ^3J(H,H) = 7.0 Hz, 2H; H11), 7.25−7.21 (m, 6H; H4, H6, H12), 7.11 (t, ^3J(H,H) = 7.5 Hz, 2H; H5). ^{13}C{^{1}H} NMR (125.78 MHz, CD_2Cl_2, 296 K): δ 161.26 (C1), 145.76 (C9), 143.46 (C8), 141.55 (C3), 134.23 (C11), 133.57 (C10), 131.93 (C13), 129.81 (C2), 128.58 (C12), 125.36 (C5), 124.77 (C6), 124.66 (C4), 123.38 (C7), 122.43 (C14). ^{1}H−^{29}Si-HMBC NMR (400.13, 79.49 MHz, THF-d_8, 296 K): δ −24.1 (Si). HR-MS (EI): calcd for $C_{28}H_{16}S_2Si$ 444.0463, found 444.0457. Mp 215.5 °C (decomp.). The asymmetric route is published elsewhere.[36]

*Methylsilicate (**7a**).*

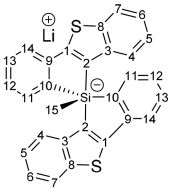

MeLi (0.084 mL. 0.135 mmol, 1.2 equiv) was added to a solution of **6** (50 mg, 0.113 mmol, 1.0 equiv) in THF (1 mL) at −78 °C. The clear yellow solution was stirred at this temperature for 15 min and warmed to room temperature to stir for another 15 min. Solvents were evaporated, and a pale yellow solid remained, which was washed using Et_2O (2,5 mL), stripped using THF, and residual solvents evaporated to obtain **7a** as a pale yellow solid (71.7 mg, 0.095 mmol, 84%). ^{1}H NMR (500.23 MHz, THF-d_8, 294 K): δ 7.80 (d, ^3J(H,H) = 8.0 Hz, 4H; H4, H7), 7.42 (d, ^3J(H,H) = 7.0 Hz, 2H; H11), 7.19 (d, ^3J(H,H) = 7.5 Hz, 2H; H14), 7.11 (t, ^3J(H,H) = 7.3 Hz, 2H; H5), 7.04 (t, ^3J(H,H) = 7.3 Hz, 4H; H6, H13), 6.69 (t, ^3J(H,H) = 7.3 Hz, 2H; H12), 0.44 (s, 3H; H15). ^{13}C{^{1}H} NMR (125.78 MHz, THF-d_8, 293 K): δ 170.02 (C2), 152.57 (C10), 148.42 (C3), 147.37 (C9), 146.54 (C1), 145.37 (C8), 137.94 (C11), 128.45 (C13), 127.70 (C4), 124.80 (C12), 123.30 (C5), 122.60 (C7), 122.09 (C6), 120.11 (C14), 7.03 (C15). ^{1}H−^{29}Si-HMBC NMR (400.13, 79.49 MHz, THF-d_8, 296 K): δ −111.7. HR-MS (ESI): calcd for $C_{29}H_{19}S_2Si$ 459.0703, found 459.0735. Mp 37.4 °C (decomp.).

*Ethylsilicate (**7b**).*

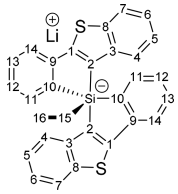

EtLi (0.24 mL. 0.118 mmol, 1.1 equiv) was added to a solution of **6** (50 mg, 0.113 mmol, 1.0 equiv) in THF (1 mL) at −78 °C. The slightly pale suspension was stirred at this temperature for 15 min and warmed to room temperature to stir for another 15 min. Solvents were evaporated *in vacuo* to obtain **7b** as a pale yellow foam (73.7 mg, 0.096 mmol, 85%). ^{1}H NMR (500.23 MHz, one drop of DMF in THF-d_8, 294 K): δ 7.86 (d, ^3J(H,H) = 8.0 Hz, 2H; H4), 7.81 (d, ^3J(H,H) = 8.0 Hz, 2H; H7), 7.47 (d, ^3J(H,H) = 7.0 Hz, 2H; H11), 7.19 (d, ^3J(H,H) = 7.0 Hz, 2H; H14), 7.11 (t, ^3J(H,H) = 7.3 Hz, 2H; H5), 7.04 (t, ^3J(H,H) = 7.3 Hz, 4H; H6, H13), 6.70 (t, ^3J(H,H) = 7.3 Hz, 2H; H12), 1.16−1.12 (m, 1H; H15$_{eq}$), 0.90−0.84 (m, 1H; H15$_{ax}$), 0.68 (t, ^3J(H,H) = 8.0 Hz, 3H; H16). ^{13}C{^{1}H} NMR (125.78 MHz, one drop of DMF in THF-d_8, 293 K): δ 169.37 (C2), 151.68 (C10), 148.64 (C3), 147.58 (C9), 147.08 (C1), 145.29 (C8), 138.18 (C11), 128.48 (C13), 127.88 (C4), 124.89 (C12), 123.23 (C5), 122.56 (C7), 121.99 (C6), 120.10 (C14), 15.90 (C15), 9.75 (C16). ^{1}H−^{29}Si-HMBC NMR (400.13, 79.49 MHz, THF-d_8, 296 K): δ −102.1. HR-MS (ESI): calcd for $C_{30}H_{21}S_2SiO$ 489.0803, found 489.0827.

*Phenylsilicate (**7c**).*

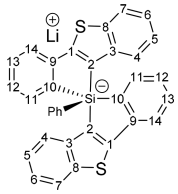

PhLi (0.07 mL. 0.14 mmol, 1.2 equiv) was added to a solution of **6** (50 mg, 0.113 mmol, 1.0 equiv) in THF (1 mL) at −78 °C. The brown solution was stirred at this temperature for 15 min and warmed to room temperature to stir for another 15 min. Solvents were evaporated, and a pale brown solid remained, which was washed using Et_2O (2,5 mL), stripped using THF, and residual solvents were evaporated to obtain **7c** as a pale white solid (73.6 mg, 0.90 mmol, 80%). ^{1}H NMR (500.23 MHz, THF-d_8, 294 K): δ 7.88 (d, ^3J(H,H) = 8.0 Hz, 2H; H7), 7.37 (d, ^3J(H,H) = 8.0 Hz, 4H; H11, H14), 7.26−7.22 (m, 4H; H4, H13), 7.18−7.16 (m, 2H; *o*-PhH), 7.04 (t, ^3J(H,H) = 7.5 Hz, 2H; H6), 6.94 (t, ^3J(H,H), 2H, H5), 6.82−6.78 (m, 5H, H12, *m*-PhH, *p*-PhH). ^{13}C{^{1}H} NMR (125.78 MHz, THF-d_8, 293 K): δ 168.21 (C2), 151.58 (*ipso*-PhC), 150.65 (C10), 147.76 (C3), 147.66 (C9), 146.77 (C1), 144.76 (C8), 137.90 (C11), 133.66 (*m*-PhC), 129.69 (C13), 127.47 (C4), 127.08 (*o*-PhC), 125.47 (*p*-PhC), 125.39 (C12), 123.59 (C5), 122.98 (C7), 122.70 (C6), 120.60 (C14). ^{1}H−^{29}Si-HMBC NMR (400.13, 79.49 MHz, THF-d_8, 296 K): δ −107.5. HR-MS (ESI): calcd for $C_{34}H_{21}S_2Si$ 521.0859, found 521.0842. Mp 59.4 °C (decomp.).

DOI: 10.1021/acs.inorgchem.8b01861
Inorg. Chem. 2018, 57, 12697−12708

1-Bromo-2-naphthyl Trifluoromethanesulfonate.[17] Using a modified method from Jarvest et al., triflic anhydride (81.6 mmol, 13.72 mL, 1.2 equiv) was added dropwise to a solution of 1-bromo-2-naphthyl (68.0 mmol, 15.16 g, 1.0 equiv) in 100 mL of pyridine at 0 °C. After 5 min, the red reaction mixture was warmed to room temperature and stirred overnight. The reaction mixture was washed with water, extracted with Et_2O (3×), and the combined organic layers washed with brine, dried over $MgSO_4$, filtered, and concentrated *in vacuo*. The resulting brown oil was purified via flash column chromatography (*c*-hexane/EtOAc = 19:1), resulting in an yellow oil that crystallized upon cooling overnight at −5 °C, resulting in off-white crystals (23.2 g, 96%). ^{1}H NMR (500.23 MHz, $(CD_3)_2SO$, 296 K): δ 8.23 (d, ^3J(H,H) = 8.5 Hz, 1H), 8.19 (d, ^3J(H,H) = 9.1 Hz, 1H), 8.12 (d, ^3J(H,H) = 7.9 Hz, 1H), 7.81 (t, ^3J(H,H) = 7.7 Hz, 1H), 7.73 (t, ^3J(H,H) = 7.6 Hz, 1H), 7.66 (d, ^3J(H,H) = 9.1 Hz, 1H). Mp 32.2 °C.

*2-(2-Bromophenyl)-1-bromonaphthalene (**8**).*

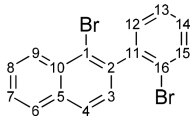

A solution of 1-bromo-2-naphthyl trifluoromethanesulfonate (1.5 mmol, 0.53 g, 1.0 equiv), 2-bromophenylboronic acid (1.5 mmol, 0.30 g, 1.0 equiv), $Pd(PPh_3)_4$ (0.075 mmol, 86.7 mg, 0.05 equiv), and Na_2CO_3 (4.5 mmol, 0.48 g, 3.0 equiv) in 10 mLof 1,4-dioxane and 10 mL of water was heated to 100 °C and stirred overnight (18 h) under a nitrogen atmosphere. The resulting black suspension was washed with 2 M HCl and then brine and subsequently extracted with EtOAc. The combined organic layers were dried over $MgSO_4$, filtered, and concentrated *in vacuo*, resulting in a brown oil. The product was purified via flash column chromatography (*c*-hexane), and the colorless oil was recrystallized from pentane, resulting in colorless crystals (0.180 g, 0.50 mmol, 33%). ^{1}H NMR (500.23 MHz, $(CD_3)_2SO$, 296 K): δ 8.27 (d, ^3J(H,H) = 8.3 Hz, 1H; H9), 8.07−8.04 (m, 2H; H4 and H6), 7.78 (dd, ^3J(H,H) = 8.0 Hz, ^4J(H,H) = 0.8 Hz, 1H; H15), 7.74 (td, ^3J(H,H) = 7.0 Hz, ^4J(H,H) = 1.3 Hz 1H; H8), 7.67 (td, ^3J(H,H) = 8.0 Hz, ^4J(H,H) = 1.0 Hz 1H; H7), 7.51 (td, ^3J(H,H) = 7.6 Hz, ^4J(H,H) = 1.3 Hz, 1H; H13), 7.42−7.37 (m, 3H; H12, H3, and H14). ^{13}C{^{1}H} NMR (125.8 MHz, $(CD_3)_2SO$, 296 K): δ 142.33 (C11), 139.92 (C2), 133.53 (C5), 132.41 (C15), 131.41 (C10), 131.07 (C14), 129.97 (C12), 128.49 (C6), 128.32 (C8), 127.89 (C4), 127.88 (C3), 127.76 (C13), 127.20 (C8), 126.85 (C9), 122.59 (C1), 122.50 (C16). IR (neat): 3053 (w, C−H_{Ar}), 1022 (m, C−Br), 955 (m, C−Br), 818 (m, C_{Ar}−H), 750 (s, C_{Ar}−H). HR-MS (EI): calcd for $C_{16}H_{10}Br_2$ 361.9129, found 361.9129. Mp 69.8−73.0 °C.

*Bis(2-phenylnaphthalene-2,1′-diyl)-silane (**9**).*

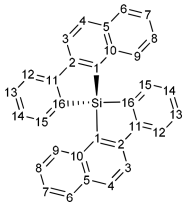

n-BuLi (1.6M, 4.51 mmol, 2.82 mL, 2.05 equiv) was added to a solution of **8** (2.2 mmol, 0.80 g, 1.0 equiv) in 10 mL of diethyl ether at −78 °C, and the resulting yellow solution was stirred for 1 h at −78 °C. The reaction mixture was warmed up to room temperature, and $SiCl_4$ (1.1 mmol, 0.17 mL, 0.5 equiv) added at 0 °C, and the resulting white suspension stirred overnight (17 h) at room temperature. The reaction mixture was washed with 2 M HCl, then water and brine, and subsequently extracted into DCM. The combined organic layers were dried over $MgSO_4$, filtered, and concentrated *in vacuo*. The resulting colorless solid was further purified using flash column chromatography (*c*-hexane/EtOAc = 99:1 → 49:1), which after evaporation of all volatiles resulted in (blue fluorescent) colorless crystals that were washed with pentane and dried *in vacuo* (0.33 g, 0.76 mmol, 69%). ^{1}H NMR (500.23 MHz, CD_2Cl_2, 296 K): δ 8.21 (d, ^3J(H,H) = 8.8 Hz, 2H; H3), 8.13 (d, ^3J(H,H) = 7.6 Hz, 2H; H12), 8.09 (d, ^3J(H,H) = 8.5 Hz, 2H; H4), 7.81 (d, ^3J(H,H) = 8.2 Hz, 2H; 6H), 7.60 (t, ^3J(H,H) = 7.7 Hz, 2H; H13), 7.43 (d, ^3J(H,H) = 6.9 Hz, 2H; H15), 7.29−7.23 (m, 4H; H7 and H14), 7.16 (d, ^3J(H,H) = 8.2 Hz, 2H; H9), 7.06 (t, ^3J(H,H) = 7.6 Hz, 2H; H8). ^{13}C{^{1}H} NMR (125.78 MHz, CD_2Cl_2, 296 K): δ 150.42 (C11), 149.81 (C2), 137.47 (C10), 134.54 (C15), 133.66 (C5), 133.17 (C16), 132.70 (C4), 131.90 (C13), 131.40 (C1), 128.88 (C6), 128.66 (C9), 128.55 (C14), 127.43 (C8), 126.23 (C7), 122.09 (C12), 120.43 (C3). ^{1}H−^{29}Si-HMBC NMR (400.13, 79.49 MHz, CD_2Cl_2, 296 K): δ −8.64; IR (neat): 3040 (w, C−H_{Ar}), 820 (m, C_{Ar}−H), 758 (s, C_{Ar}−H). HR-MS (EI): calcd for $C_{32}H_{20}Si$ 432.1334, found 432.1330. Mp 275.7 °C (decomp.). The asymmetric route is published elsewhere.[36]

*Bis(2-phenylnaphthalene-2,1′-diyl)-methylsilicate (**10a**).*

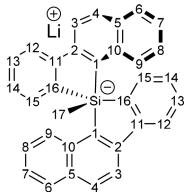

MeLi (1.6 M, 0.139 mmol, 0.09 mL, 1.1 equiv) was added to a solution of bis(2-phenylnaphthalene-2,1′-diyl)silane (**9**) (0.116 mmol, 50 mg, 1.0 equiv) in dry THF (1 mL) at −78 °C, and afterward, the yellow solution was stirred for 30 min at this temperature and 30 min at room temperature. All volatiles were removed from the clear yellow solution *in vacuo*, and the resulting residue was washed with pentane (3 mL), stripped with THF (1 mL), and dried *in vacuo* yielding **6a** as a yellow solid (88.27 mg, 0.11 mmol, 96%). ^{1}H NMR (500.23 MHz, THF-d_8, 293 K): δ 8.23 (d, ^3J(H,H) = 8.3 Hz, 2H; H9), 8.00 (d, ^3J(H,H) = 8.3 Hz, 2H; H3), 7.80 (d, ^3J(H,H) = 7.6 Hz, 2H; H12), 7.69 (d, ^3J(H,H) = 8.2 Hz, 2H; H6), 7.56 (d, ^3J(H,H) = 8.5 Hz, 2H; H4), 7.31 (d, ^3J(H,H) = 6.9 Hz, 2H; H15), 7.15 (t, ^3J(H,H) = 6.9 Hz, 2H; H7), 7.08 (t, ^3J(H,H) = 7.1 Hz, 4H; H8, H13), 6.61 (t, ^3J(H,H) = 6.9 Hz, 2H; H14) 0.49 (s, 3H; H17). ^{13}C{^{1}H} NMR (125.78 MHz, THF-d_8, 293 K): δ 168.66 (C1), 150.11 (C16), 149.88 (C11), 141.02 (C2), 139.87 (C10), 139.17 (C15), 134.10 (C9), 133.76 (C5), 128.28 (C6), 128.15 (C13), 125.40 (C4), 124.37 (C14), 123.15 (C7), 123.02 (C8), 119.87 (C3), 118.80 (C12), 10.85 (C17). ^{1}H−^{29}Si-HMBC NMR (400.13, 79.49 MHz, THF/THF-d_8, 295 K): δ −95.0 (Si). HR-MS (ESI): calcd for $C_{33}H_{23}Si$ 447.1575, found 447.1595. Mp 33.7 °C (decomp.).

*Lithium Bis(2-phenylnaphthalene-2,1′-diyl)ethylsilicate (**10b**).*

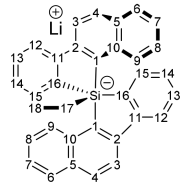

EtLi (0.5 M, 0.122 mmol, 0.24 mL, 1.05 equiv) was added to a solution of **9** (0.116 mmol, 50 mg, 1.0 equiv) in dry THF (1 mL) at −78 °C, and the brownish/red solution was stirred for 30 min at this temperature and 30 min at room temperature. Afterward, all volatiles were removed *in vacuo* yielding **6b** as a pale yellow foam (93.43 mg, 0.12 mmol, quant.). ^{1}H NMR (500.23 MHz, THF-d_8, 293 K): δ 8.28 (d, ^3J(H,H) = 8.3 Hz, 2H; H9), 8.00 (d, ^3J(H,H) = 8.3 Hz, 2H; H3), 7.80 (d, ^3J(H,H) = 7.4 Hz, 2H; H12), 7.70 (d, ^3J(H,H) = 8.0 Hz, 2H; H6), 7.57 (d, ^3J(H,H) = 8.3 Hz, 2H; H4), 7.36 (d, ^3J(H,H) = 7.1 Hz, 2H; H15), 7.18−7.16 (m, 2H; H7), 7.12−7.07 (m, 4H; H8, H13), 6.61 (t, ^3J(H,H) = 7.1 Hz, 2H; H14), 1.34 (dq, ^2J(H,H) = 13.1 Hz, ^3J(H,H) = 5.0 Hz, 1H; $H17_{eq}$), 0.88 (dq, ^2J(H,H) = 13.4 Hz, ^3J(H,H) = 6.4 Hz, 1H; $H17_{ax}$), 0.33 (t, ^3J(H,H) = 7.4 Hz, 3H; H18). ^{13}C{^{1}H} NMR (125.78 MHz, THF-d_8, 293 K): δ 167.19 (C1), 149.34 (C11), 148.29 (C16), 140.92 (C2), 138.96 (C10), 138.39 (C15), 132.76 (C9), 132.58 (C5), 127.20 (C6), 126.99 (C13), 124.31 (C4), 123.25 (C14), 122.10 (C7), 121.96 (C8), 118.52 (C3), 117.61 (C12), 16.77 (C17), 8.95 (C18). ^{1}H−^{29}Si-HMBC NMR (400.13, 79.49 MHz,

DOI: 10.1021/acs.inorgchem.8b01861
Inorg. Chem. 2018, 57, 12697−12708

THF-d_8, 296 K): δ −95.06. HR-MS (ESI): calcd. for $C_{34}H_{25}OSi$ 477.1680, found 477.1702.

*Lithium Bis(2-phenylnaphthalene-2,1′-diyl)phenylsilicate (**10c**).*

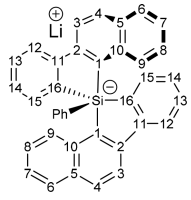

PhLi (1.9 M, 0.139 mmol, 0.07 mL, 1.2 equiv) was added to a solution of bis(2-phenylnaphthalene-2,1′-diyl)silane (**9**) (0.116 mmol, 50 mg, 1.0 equiv) in dry THF (1 mL) at −78 °C, and afterward, the brownish/red solution was stirred for 30 min at this temperature and 30 min at room temperature. All volatiles were removed *in vacuo*, and the resulting residue was washed with Et_2O (2,5 mL) and dried *in vacuo*, yielding **10c** as a yellowish solid (78.63 mg, 0.98 mmol, 84%). The solid was suspended in 0.7 mL of THF-d_8, and two drops of dry DMF were added to promote solvation allowing NMR measurements. ^{1}H NMR (500.23 MHz, THF-d_8, 294 K): δ 8.05 (d, ^3J(H,H) = 8.5 Hz, 2H; H3), 7.88 (d, ^3J(H,H) = 7.5 Hz, 2H; H12), 7.71 (d, ^3J(H,H) = 8.0 Hz, 2H; H9), 7.60−7.56 (m, 4H; H4, H6), 7.14 (d, ^3J(H,H) = 7.0 Hz, 2H; H14), 7.11 (t, ^3J(H,H) = 7.5 Hz, 2H; H13), 6.97−6.96 (m, 4H; H7, *o*-PhH), 6.68 (t, ^3J(H,H) = 7.5 Hz, 2H; H8), 6.58 (t, ^3J(H,H) = 7.0 Hz, 2H; H14), 6.54−6.48 (m, 3H; *p*-PhH, *m*-PhH). ^{13}C{^{1}H} NMR (125.78 MHz, THF-d_8, 293 K): δ 166.56 (C1), 156.09 (*ipso*-PhC), 150.85 (C11), 148.50 (C16), 141.80 (C2), 139.70 (C10), 139.38 (C15), 135.61 (*o*-PhC), 133.95 (C9), 133.62 (C5), 128.41 (C13), 127.75 (C6), 125.96 (C4), 125.90 (*m*-PhC), 124.57 (C14), 124.09 (*p*-PhC), 123.02 (C7), 122.80 (C8), 119.17 (C3) 118.84 (C12). ^{1}H−^{29}Si-HMBC NMR (400.13, 79.49 MHz, THF/THF-d_8, 295 K): δ −99.47. HR-MS (ESI): calcd for $C_{38}H_{25}Si$ 509.1731, found 509.1709.

*Tetramethylammonium Fluorosilicate (**10d**).*

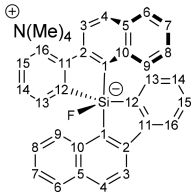

Tetramethylammonium fluoride (21.5 mg, 0.23 mmol, 2.0 equiv) was dried under dynamic vacuum for 3 h at 148 °C. **9** (50 mg, 0.116 mmol, 1.0 equiv) was dissolved in DMF separately and layered on top of tetramethylammonium fluoride. The yellowish suspension was stirred for 30 min and filtered afterward. The clear yellow filtrate was concentrated *in vacuo* to yield **10d** as a white solid (quant.). ^{1}H NMR (400.1 MHz, DMF-d_7, 294 K): δ 8.22 (d, ^3J(H,H) = 9.9 Hz, 2H; H9), 8.03 (dd, ^3J(H,H) = 8.8 Hz, ^4J(H,H) = 2.0 Hz, 1H; H3), 7.80 (d, ^3J(H,H) = 8.0 Hz, 4H; H6, H16), 7.73 (d, ^3J(H,H) = 8.4 Hz, 2H; H4), 7.25 (t, ^3J(H,H) = 6.8 Hz, 2H; H7), 7.16 (t, ^3J(H,H) = 8.0 Hz, 2H; H8), 7.08 (dt, ^3J(H,H) = 7.4 Hz, ^4J(H,H) = 1.4 Hz, 2H; H15), 6.60 (dd, ^3J(H,H) = 7.0 Hz, ^4J(H,H) = 0.8 Hz, 2H; H13), 6.54 (dt, ^3J(H,H) = 7.1 Hz, ^4J(H,H) = 0.8 Hz, 2H; H14), 3.34 (s, 12H, NMe_4). ^{13}C{^{1}H} NMR (100.6 MHz, DMF-d_7, 293 K): δ 160.28 (C1), 150.51 (C11), 148.87 (C12), 141.94 (C2), 139.66 (C10), 137.15 (C13), 134.15 (C9, C5), 129.62 (C15), 128.92 (C6), 127.14 (C4), 125.81 (C14), 124.69 (C8), 124.64 (C7), 120.24 (C3), 119.72 (C16). ^{1}H−^{29}Si-HMBC NMR (400.13, 79.49 MHz, DMF-d_7, 296 K): δ −81.31 (d, ^1J(Si,F) = 287.8 Hz). ^{19}F{^{1}H} NMR (235.3 MHz, DMF-d_7): δ −109.99 (^1J(F,Si) = 289.3 Hz).

*Tetrabutylammonium Fluorosilicate (**10e**).*

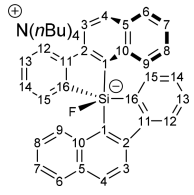

TBAF (0.12 mL, 0.12 mmol, 1.04 equiv, 1.0 M in THF) was added to a solution of **9** (50 mg, 0.116 mmol, 1.0 equiv) in THF (1 mL) at room temperature. The yellow solution was stirred at this temperature for 30 min and solvents were evaporated afterward until a yellow foam remained, which was washed with Et_2O (2,5 mL) yielding **10e** as a yellow foam (quant.). ^{1}H NMR (400.1 MHz, THF-d_8, 294 K): δ 8.20 (d, ^3J(H,H) = 8.0 Hz, 2H; 9H), 7.98 (d, ^3J(H,H) = 8.4 Hz, 2H; 3H), 7.72 (d, ^3J(H,H) = 7.6 Hz, 4H; 6H, 12H), 7.66 (d, ^3J(H,H) = 8.4 Hz, 2H; 4H), 7.20−7.17 (m, 2H; 7H), 7.09 (t, ^3J(H,H) = 7.4 Hz, 2H; 8H), 7.03 (t, ^3J(H,H) = 7.4 Hz, 2H; 13H), 6.66 (d, ^3J(H,H) = 7.2 Hz, 2H; 15H), 6.34 (t, ^3J(H,H) = 7.0 Hz, 2H; 14H), 2.73−2.69 (m, 8H; N(CH_2Pr)$_4$), 1.25−1.17 (m, 8H; N($CH_2C\mathit{H}_2$Et)$_4$, 1.07−0.98 (m, 8H; N($CH_2CH_2C\mathit{H}_2$Me)$_4$, 0.76 (t, ^3J(H,H) = 7.3 Hz, 12H; $CH_2CH_2CH_2C\mathit{H}_3$). ^{13}C{^{1}H} NMR (100.6 MHz, THF-d_8, 293 K): δ 160.38 (d, ^2J(C,F) = 101.9 Hz, C1), 150.03 (C11), 148.17 (C16), 142.00 (C2), 139.39 (C10), 137.31 (C15), 134.32 (C9), 134.10 (C5), 128.78 (C13), 128.44 (C6), 126.43 (C4), 125.51 (C14), 123.59 (C8), 123.72 (C7), 119.84 (C3), 118.95 (C12), 58.73 (CH_2), 24.17 (CH_2), 20.09 (CH_2), 13.75 (CH_3). ^{1}H−^{29}Si-HMBC NMR (400.13, 79.49 MHz, THF-d_8, 296 K): δ −88.80 (d, ^1J(Si,F) = 283.8 Hz). ^{19}F{^{1}H} NMR (235.3 MHz, THF-d_8): δ −107.04 (^1J(F,Si) = 287.0 Hz, ^2J(F,C) = 101.9 Hz). HR-MS (CSI): calcd for $C_{32}H_{20}FSi$ 451.1318, found 451.1297.

*11-(2-(Naphthalen-2-yl)phenyl)-11-phenyl-11H-benzo[b]-naphtho[2,1-d]silole (**11**).*

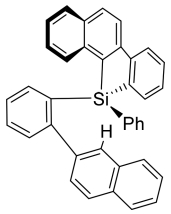

PhLi (1.9 M, 0.81 mmol, 0.04 mL, 1.1 equiv) was added to a solution of bis(2-phenylnaphthalene-2,1′-diyl)silane (**9**) (0.074 mmol, 32 mg, 1.0 equiv) in dry THF (1 mL) at −78 °C, and afterward, the brownish/red solution was stirred for 30 min at this temperature and 30 min at room temperature. All volatiles were removed *in vacuo* and the resulting residue was washed with Et_2O (2,5 mL) and dried *in vacuo*. The residue was dissolved in THF (3 mL) and water (3 drops) was added to the yellow solution. All volatiles were evaporated to yield the product of >90% purity as a white foam (53 mg). ^{1}H NMR (400.1 MHz, CD_2Cl_2, 294 K): δ 7.93 (d, ^3J(H,H) = 7.4 Hz, 1H), 7.78−7.72 (m, 2H), 7.65−7.60 (m, 3H), 7.54 (t, ^3J(H,H) = 7.4 Hz, 1H), 7.48−7.19 (m, 14H), 7.11 (t, ^3J(H,H) = 7.2 Hz, 1H), 7.02 (d, ^3J(H,H) = 8.3 Hz, 1H), 6.98 (s, 1H), 6.87 (d, ^3J(H,H) = 8.1 Hz, 1H), 6.79 (d, ^3J(H,H) = 8.3 Hz, 1H). ^{13}C{^{1}H} NMR (100.6 MHz, CD_2Cl_2, 293 K): 151.47 (q), 148.34 (q), 147.41 (q), 140.08 (q), 138.55 (CH), 137.65 (q), 136.68 (q), 136.03 (2CH), 135.31 (q), 134.29 (q), 133.42 (CH), 133.37 (q), 132.51 (q), 132.18 (q), 132.00 (q), 130.88 (CH), 130.45 (CH), 130.17 (CH), 130.07 (CH), 130.05 (CH), 129.52 (CH), 129.02 (CH), 128.60 (CH), 128.42 (2CH), 128.15 (CH), 127.58 (CH), 127.28 (2CH), 127.04 (CH), 126.88 (CH), 126.44 (CH), 125.83 (CH), 125.71 (CH), 125.64 (CH), 121.38 (CH), 120.00 (CH). ^{1}H−^{29}Si-HMBC NMR (400.13, 79.49 MHz, CD_2Cl_2, 296 K): δ −10.40. HR-MS (FD): calcd for $C_{38}H_{26}FSi$ 510.18038, found 510.18183.

■ ASSOCIATED CONTENT

Supporting Information

The Supporting Information is available free of charge on the ACS Publications website at DOI: 10.1021/acs.inorgchem.8b01861.

All ^{1}H, ^{13}C, and ^{1}H−^{29}Si-HMBC NMR spectra. Geometries of computed structures. X-ray crystallographic data for **7c**, Δ-**9**, Λ-**10c**, and **10e** (PDF)

Accession Codes

CCDC 1853537−1853540 contain the supplementary crystallographic data for this paper. These data can be obtained

DOI: 10.1021/acs.inorgchem.8b01861
Inorg. Chem. 2018, 57, 12697−12708

free of charge via www.ccdc.cam.ac.uk/data_request/cif, or by emailing data_request@ccdc.cam.ac.uk, or by contacting The Cambridge Crystallographic Data Centre, 12 Union Road, Cambridge CB2 1EZ, UK; fax: +44 1223 336033.

AUTHOR INFORMATION

Corresponding Authors

*E-mail: A.W.Ehlers@uva.nl.

*E-mail: K.Lammertsma@vu.nl.

ORCID

J. Chris Slootweg: 0000-0001-7818-7766

Koop Lammertsma: 0000-0001-9162-5783

Notes

The authors declare no competing financial interest.

ACKNOWLEDGMENTS

This work was supported by The Netherlands Organisation for Scientific Research, Chemical Sciences (NWO−CW). We acknowledge SARA Computing and Networking Services for computer time.

REFERENCES

(1) van 't Hoff, J. H. *Arch. Neerl. Sci. Exactes Nat.* **1874**, *9*, 445−454.

(2) Meijer, E. W. Jacobus Henricus van 'T Hoff; Hundred Years of Impact on Stereochemistry in the Netherlands. *Angew. Chem., Int. Ed.* **2001**, *40* (20), 3783−3789.

(3) Federsel, H.-J. Stereoselective Synthesis of Drugs − An Industrial Perspective. In *Chirality in Drug Research*; Francotte, E., Lindner, W., Eds.; Wiley-VCH Verlag GmbH & Co. KGaA, 2006; pp 27−65.

(4) Itsuno, S. *Polymeric Chiral Catalyst Design and Chiral Polymer Synthesis* [Online]; Wiley, 2011. http://eu.wiley.com/WileyCDA/WileyTitle/productCd-0470568208.html (accessed August 28, 2016).

(5) *Dynamic Stereochemistry of Chiral Compounds*; Royal Society of Chemistry: Cambridge, U.K., 2007.

(6) Feringa, B. L.; van Delden, R. A. Absolute Asymmetric Synthesis: The Origin, Control, and Amplification of Chirality. *Angew. Chem., Int. Ed.* **1999**, *38* (23), 3418−3438.

(7) Huo, H.; Fu, C.; Harms, K.; Meggers, E. Asymmetric Catalysis with Substitutionally Labile yet Stereochemically Stable Chiral-at-Metal Iridium(III) Complex. *J. Am. Chem. Soc.* **2014**, *136* (8), 2990−2993.

(8) Gong, L.; Chen, L.-A.; Meggers, E. Asymmetric Catalysis Mediated by the Ligand Sphere of Octahedral Chiral-at-Metal Complexes. *Angew. Chem., Int. Ed.* **2014**, *53* (41), 10868−10874.

(9) Martin, O. Chirality Transfer from Silicon to Carbon. *Chem. - Eur. J.* **2005**, *12* (1), 30−37.

(10) Chen, P. Designing Sequence Selectivity into a Ring-Opening Metathesis Polymerization Catalyst. *Acc. Chem. Res.* **2016**, *49* (5), 1052−1060.

(11) Bauer, E. B. Chiral-at-Metal Complexes and Their Catalytic Applications in Organic Synthesis. *Chem. Soc. Rev.* **2012**, *41* (8), 3153−3167.

(12) Brunner, H. Optically Active Organometallic Compounds of Transition Elements with Chiral Metal Atoms. *Angew. Chem., Int. Ed.* **1999**, *38* (9), 1194−1208.

(13) Bassindale, A. R.; Glynn, S. J.; Taylor, P. G. Reaction Mechanisms of Nucleophilic Attack at Silicon. In *Patai's Chemistry of Functional Groups*; Wiley, 2009.

(14) Berry, R. S. Correlation of Rates of Intramolecular Tunneling Processes, with Application to Some Group V Compounds. *J. Chem. Phys.* **1960**, *32* (3), 933−938.

(15) Berry, R. S. Time-Dependent Measurements and Molecular Structure: Ozone. *Rev. Mod. Phys.* **1960**, *32* (2), 447−454.

(16) Bauer, J. O.; Strohmann, C. Stereocontrol in Nucleophilic Substitution Reactions at Silicon: The Role of Permutation in Generating Silicon-Centered Chirality. *J. Am. Chem. Soc.* **2015**, *137* (13), 4304−4307.

(17) Kojima, S.; Nakamoto, M.; Akiba, K. Stereospecific Pseudorotation of Diastereomeric Anti-Apicophilic Spirophosphoranes: A Novel Stereochemical Transformation Involving 10-P-5 Phosphoranes. *Eur. J. Org. Chem.* **2008**, *2008* (10), 1715−1722.

(18) Kojima, S.; Nakamoto, M.; Matsukawa, S.; Akiba, K. Stereomutation of a Diastereomeric Pair of 10-P-5 Hydroxyphosphoranes. *Heteroat. Chem.* **2011**, *22* (3−4), 491−499.

(19) Kojima, S.; Kajiyama, K.; Nakamoto, M.; Akiba, K. First Characterization of a 10-P-5 Spirophosphorane with an Apical Carbon−Equatorial Oxygen Ring. Kinetic Studies on Pseudorotation of Stereoisomers. *J. Am. Chem. Soc.* **1996**, *118* (50), 12866−12867.

(20) Kojima, S.; Kajiyama, K.; Akiba, K. Characterization of Enantiomeric Pairs of Optically Active 10-P-5 Phosphoranes with Asymmetry Only at Phosphorus. *Bull. Chem. Soc. Jpn.* **1995**, *68* (7), 1785−1797.

(21) Böhme, U.; Fels, S. A New Type of Chiral Pentacoordinated Silicon Compounds with Azomethine Ligands Made from Acetylacetone and Amino Acids. *Inorg. Chim. Acta* **2013**, *406*, 251−255.

(22) Stevenson, W. H.; Wilson, S.; Martin, J. C.; Farnham, W. B. Pseudorotational Mechanism for the Inversion of 10-Si-5 Siliconates: Ligand Structure and Reactivity. *J. Am. Chem. Soc.* **1985**, *107* (22), 6340−6352.

(23) Couzijn, E. P. A.; Slootweg, J. C.; Ehlers, A. W.; Lammertsma, K. Stereomutation of Pentavalent Compounds: Validating the Berry Pseudorotation, Redressing Ugi's Turnstile Rotation, and Revealing the Two- and Three-Arm Turnstiles. *J. Am. Chem. Soc.* **2010**, *132* (51), 18127−18140.

(24) Meakin, P.; Muetterties, E. L.; Jesson, J. P. Intramolecular Rearrangement Mechanisms in Five-Coordinate Complexes. *J. Am. Chem. Soc.* **1972**, *94* (15), 5271−5285.

(25) Muetterties, E. L. Topological Representation of Stereoisomerism. I. Polytopal Rearrangements. *J. Am. Chem. Soc.* **1969**, *91* (7), 1636−1643.

(26) Couzijn, E. P. A.; Schakel, M.; de Kanter, F. J. J.; Ehlers, A. W.; Lutz, M.; Spek, A. L.; Lammertsma, K. Dynamic Configurational Isomerism of a Stable Pentaorganosilicate. *Angew. Chem., Int. Ed.* **2004**, *43* (26), 3440−3442.

(27) Couzijn, E. P. A.; van den Engel, D. W. F.; Slootweg, J. C.; de Kanter, F. J. J.; Ehlers, A. W.; Schakel, M.; Lammertsma, K. Configurationally Rigid Pentaorganosilicates. *J. Am. Chem. Soc.* **2009**, *131* (10), 3741−3751.

(28) de Keijzer, A. H. J. F.; de Kanter, F. J. J.; Schakel, M.; Osinga, V. P.; Klumpp, G. W. New Directions in Organometallic ChemistryIn Search of Stable Lithium Pentaorganylsilicates; Special Role of Five Phenyl Ligands and of Ligands Containing the 1,4-(1,3-Butadiene-diyl) Unit. *J. Organomet. Chem.* **1997**, *548* (1), 29−32.

(29) Deerenberg, S.; Schakel, M.; de Keijzer, A. H. J. F.; Kranenburg, M.; Lutz, M.; Spek, A. L.; Lammertsma, K. Tetraalkylammonium Pentaorganosilicates: The First Highly Stable Silicates with Five Hydrocarbon Ligands. *Chem. Commun.* **2002**, *4*, 348−349.

(30) Ehrlich, S.; Moellmann, J.; Grimme, S. Dispersion-Corrected Density Functional Theory for Aromatic Interactions in Complex Systems. *Acc. Chem. Res.* **2013**, *46* (4), 916−926.

(31) Moberg, C. Stereomutation in Trigonal-Bipyramidal Systems: A Unified Picture. *Angew. Chem., Int. Ed.* **2011**, *50* (44), 10290−10292.

(32) Couzijn, E. P. A.; Ehlers, A. W.; Schakel, M.; Lammertsma, K. Electronic Structure and Stability of Pentaorganosilicates. *J. Am. Chem. Soc.* **2006**, *128* (41), 13634−13639.

(33) Farnham, W. B.; Harlow, R. L. Stereomutation at Pentacoordinate Silicon by Intramolecular Ligand Exchange. *J. Am. Chem. Soc.* **1981**, *103* (15), 4608−4610.

(34) Hassan, Z.; Hussain, M.; Villinger, A.; Langer, P. Synthesis of Aryl-Substituted Naphthalenes by Chemoselective Suzuki−Miyaura Reactions of Bromo-Trifluoromethanesulfonyloxy-Naphthalenes. Influence of Steric and Electronic Parameters. *Tetrahedron* **2012**, *68* (31), 6305−6313.

DOI: 10.1021/acs.inorgchem.8b01861
Inorg. Chem. 2018, 57, 12697−12708

(35) Weymiens, W.; Zaal, M.; Slootweg, J. C.; Ehlers, A. W.; Lammertsma, K. Ladder-Type P,S-Bridged Trans-Stilbenes. *Inorg. Chem.* **2011**, *50* (17), 8516−8523.
(36) van derBoon, L. J. P.; Fuku-en, S.; Slootweg, J. C.; Lammertsma, K.; Ehlers, A. W. Toward Asymmetric Synthesis of Pentaorganosilicates. *Top. Catal.* **2018**, *61*, 674−684.
(37) Sullivan, S. A.; DePuy, C. H.; Damrauer, R. Gas-Phase Reactions of Cyclic Silanes. *J. Am. Chem. Soc.* **1981**, *103* (2), 480−481.
(38) Maggiarosa, N.; Tyrra, W.; Naumann, D.; Kirij, N. V.; Yagupolskii, Y. L. [Me3Si(CF3)F]− and [Me3Si(CF3)2]−: Reactive Intermediates in Fluoride-Initiated Trifluoromethylation with Me3-SiCF3— An NMR Study. *Angew. Chem., Int. Ed.* **1999**, *38* (15), 2252−2253.
(39) Soli, E. D.; Manoso, A. S.; Patterson, M. C.; DeShong, P.; Favor, D. A.; Hirschmann, R.; Smith, A. B. Azide and Cyanide Displacements via Hypervalent Silicate Intermediates. *J. Org. Chem.* **1999**, *64* (9), 3171−3177.
(40) Tacke, R.; Bertermann, R.; Burschka, C.; Dragota, S. A Zwitterionic Spirocyclic Pentacoordinate Silicon Compound Synthesized in Water by Si−O and Si−C Bond Cleavage. *Angew. Chem., Int. Ed.* **2005**, *44* (33), 5292−5295.
(41) Frisch, M. J.; Trucks, G. W.; Schlegel, H. B.; Scuseria, G. E.; Robb, M. A.; Cheeseman, J. R.; Scalmani, G.; Barone, V.; Mennucci, B.; Petersson, G. A.; Nakatsuji, H.; Caricato, M.; Li, X.; Hratchian, H. P.; Izmaylov, A. F.; Bloino, J.; Zheng, G.; Sonnenberg, J. L.; Hada, M.; Ehara, M.; Toyota, K.; Fukuda, R.; Hasegawa, J.; Ishida, M.; Nakajima, T.; Honda, Y.; Kitao, O.; Nakai, H.; Vreven, T.; Montgomery, J. A., Jr.; Peralta, J. E.; Ogliaro, F.; Bearpark, M.; Heyd, J. J.; Brothers, E.; Kudin, K. N.; Staroverov, V. N.; Kobayashi, R.; Normand, J.; Raghavachari, K.; Rendell, A.; Burant, J. C.; Iyengar, S. S.; Tomasi, J.; Cossi, M.; Rega, N.; Millam, J. M.; Klene, M.; Knox, J. E.; Cross, J. B.; Bakken, V.; Adamo, C.; Jaramillo, J.; Gomperts, R.; Stratmann, R. E.; Yazyev, O.; Austin, A. J.; Cammi, R.; Pomelli, C.; Ochterski, J. W.; Martin, R. L.; Morokuma, K.; Zakrzewski, V. G.; Voth, G. A.; Salvador, P.; Dannenberg, J. J.; Dapprich, S.; Daniels, A. D.; Farkas, O.; Foresman, J. B.; Ortiz, J. V.; Cioslowski, J.; Fox, D. J. *Gaussian 09*, revision D.01; Gaussian, Inc.: Wallingford, CT, 2009.
(42) Ditchfield, R.; Hehre, W. J.; Pople, J. A. Self-Consistent Molecular-Orbital Methods. IX. An Extended Gaussian-Type Basis for Molecular-Orbital Studies of Organic Molecules. *J. Chem. Phys.* **1971**, *54* (2), 724−728.
(43) Hehre, W. J.; Ditchfield, R.; Pople, J. A. Self—Consistent Molecular Orbital Methods. XII. Further Extensions of Gaussian—Type Basis Sets for Use in Molecular Orbital Studies of Organic Molecules. *J. Chem. Phys.* **1972**, *56* (5), 2257−2261.
(44) Hariharan, P. C.; Pople, J. A. The Influence of Polarization Functions on Molecular Orbital Hydrogenation Energies. *Theor. Chim. Acta* **1973**, *28* (3), 213−222.
(45) Gordon, M. S. The Isomers of Silacyclopropane. *Chem. Phys. Lett.* **1980**, *76* (1), 163−168.
(46) Francl, M. M.; Pietro, W. J.; Hehre, W. J.; Binkley, J. S.; Gordon, M. S.; DeFrees, D. J.; Pople, J. A. Self-consistent Molecular Orbital Methods. XXIII. A Polarization-type Basis Set for Second-row Elements. *J. Chem. Phys.* **1982**, *77* (7), 3654−3665.
(47) Rassolov, V. A.; Pople, J. A.; Ratner, M. A.; Windus, T. L. 6-31G* Basis Set for Atoms K through Zn. *J. Chem. Phys.* **1998**, *109* (4), 1223−1229.
(48) Rassolov, V. A.; Ratner, M. A.; Pople, J. A.; Redfern, P. C.; Curtiss, L. A. 6-31G* Basis Set for Third-Row Atoms. *J. Comput. Chem.* **2001**, *22* (9), 976−984.
(49) Clark, T.; Chandrasekhar, J.; Spitznagel, G. W.; Schleyer, P. V. R. Efficient Diffuse Function-Augmented Basis Sets for Anion Calculations. III. The 3-21+G Basis Set for First-Row Elements, Li−F. *J. Comput. Chem.* **1983**, *4* (3), 294−301.
(50) Becke, A. D. Density-functional Thermochemistry. III. The Role of Exact Exchange. *J. Chem. Phys.* **1993**, *98* (7), 5648−5652.
(51) Lee, C.; Yang, W.; Parr, R. G. Development of the Colle-Salvetti Correlation-Energy Formula into a Functional of the Electron Density. *Phys. Rev. B: Condens. Matter Mater. Phys.* **1988**, *37* (2), 785−789.
(52) Stephens, P. J.; Devlin, F. J.; Chabalowski, C. F.; Frisch, M. J. Ab Initio Calculation of Vibrational Absorption and Circular Dichroism Spectra Using Density Functional Force Fields. *J. Phys. Chem.* **1994**, *98* (45), 11623−11627.
(53) Barbarella, G.; Favaretto, L.; Zanelli, A.; Gigli, G.; Mazzeo, M.; Anni, M.; Bongini, A. V-Shaped Thiophene-Based Oligomers with Improved Electroluminescence Properties. *Adv. Funct. Mater.* **2005**, *15* (4), 664−670.

DOI: 10.1021/acs.inorgchem.8b01861
Inorg. Chem. 2018, 57, 12697−12708